Egyptian Journal of Archaeological and Restoration Studies (*EJARS*)
An international peer-reviewed journal published bi-annually
www.ejars.sohag-univ.edu.eg

Original article

CONSERVATION AND REDISPLAY OF AN ARCHAEOLOGICAL IRON AXE FROM BALLANA AND QUSTUL, EGYPTIAN NUBIA (370-500) A.D.

Bahig, F.[1], Sobhy, D.[2] & Rifai, M.[2(*)]

[1]*Inorganic Conservation dept., Egyptian Capital Museum, Ministry of Tourism & Monuments, Cairo, Egypt.*
[2]*Conservation dept, Faculty of Archaeology, Cairo Univ, Giza, Egypt.*
**E-mail address: mairifai@hotmail.com*

Article info.

Article history:
Received: 21-9-2024
Accepted: 23-6-2025
Doi: 10.21608/ejars.2025.471791

Keywords:
Axe Head
Iron
Rust
Redisplay
Ballana, Investigation
Preservation

EJARS – Vol. 15 (2) – Dec. 2025: 239-249

Abstract:

This paper discusses the examination, analysis and conservation of an iron axe head from a collection of daily life tools from the Ballana and Qustul regions in Egyptian Nubia (380-500 A.D.), which are currently displayed at the Egyptian Museum in Cairo. The iron axe head was discovered among other finds during the excavations of Walter Emery and Lawrence Kirwan between 1928 and 1934. The axe head was in a very poor and fragile condition, and required immediate intervention for conservation and treatment. Different analytical and investigation methods were performed to examine and identify the object's metallic structure and corrosion products such as Digital Light Microscope, Metallography, Scanning Electron Microscope (SEM), X-ray Diffraction (XRD), Raman spectroscopy (RS), Fourier-transform infrared spectroscopy (FTIR) and Elemental analysis using Energy Dispersive X-ray (EDX) and X-ray Fluorescence (pXRF). The results indicated that the axe head was manufactured from low-carbon steel. XRD and Raman spectroscopy revealed the presence of different types of corrosion products including iron oxides, hydroxides and chlorides namely Magnetite, Lepidocrocite, Goethite, Hematite and Akaganeite, in addition to the presence of Quartz - a component of soil deposits. Furthermore, soil minerals were clearly observed on the object's surface. The main purpose for this study is to evaluate the condition of the axe head and identify the rust components in order to select the most suitable conservation materials and technique to stabilize the object and prevent further degradation. Finally, the artifact was redisplayed in a suitable and proper way, as the current method of displaying was not suitable.

1. Introduction

A unique collection of archaeological iron artifacts including agricultural, daily life tools and weapons are displayed at the Egyptian Museum in Cairo, this collection was excavated from the archaeological site of "Ballana and Qustul" Egyptian Nubia (lower Nubia) which is located between Abu Simbel and the Sudanese border [1]. Archaeologists have divided Nubia into three civilizations: Napatan, Meroitic and X-group (Ballana and Qustul) [2]. The X-group civilization is located in the Ballana and Qustul villages in Egyptian Lower Nubia. Ballana is located on the west bank of the Nile opposite to Qustul, 300 km, south of Aswan, fig. (1) [3] and dates to around 350-600 AD in the time after the collapse of the Meroitic state and before the founding of the Christian Nubian kingdoms [4]. Although a number of travelers and archaeologist has noted the tumuli of Ballana and Qustul, they were not recognized until Ballana and Qustul excavation was conducted at the site between 1928 and 1931 by two archaeologists (Walter Emery and Lawrence P. Kirwan) [5]. The cemeteries contained a large number of excavated materials [6]. By the end of their expedition in 1934, they discovered many royal tombs which were equipped with the richest funerary goods in Nubia.

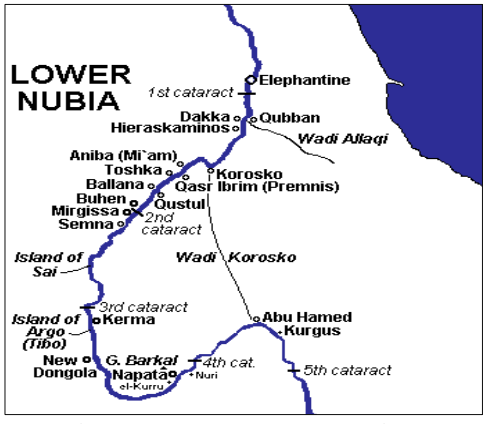

Figure (1) map of ancient Nubia showing location of Ballana and Qustul, www.touregypt.net (22/2/2024).

Bronze, iron and silver artifacts such as spears, axes, chisels and hammers were found in these tombs [7], in addition to the

remains of sacrificial horses [2,4]. Although the overall survival rate of materials from Ballana and Qustul is good, the sites (Ballana in particular) have suffered from water damage, in some cases the mud brick had become a mass of mud, so the action of the water has had a detrimental effect on the preservation rate of certain items [5]. Ancient Egypt had great mineral resources. The wide desert areas, in particular the Eastern desert, were rich in mines and quarries, which have been exploited since ancient times [7]. The iron ores of Egypt are of stratabound/ stratiform type of near surface shallow marine and subarial environment, ranging in age from early Proterozoic to Paleogene. The beginning of the iron mining process was in the Middle Bronze Age, where, iron replaced bronze and was used in the manufacture of weapons and different tools. The sporadic use of iron during the Bronze Age has been reported in Egypt and the Mediterranean, a handful of iron objects likely dates to the Old Kingdom (3rd millennium BCE), with the most ancient iron ones dated to about 3200 BCE. It is generally assumed that early iron objects were produced from meteoritic material, despite the rare existence of smelted iron fortuitously obtained as a by-product of copper and bronze. During the Bronze Age, iron was definitely rare, its value was greater than that of gold (Burney 2004), and it was primarily used for the production of ornamental, ritual, and ceremonial objects. By the end of the 2nd millennium BCE, iron had come into common use in most of the eastern Mediterranean, although the rates at which it was substituted for bronze vary from region to region [8]. Iron production involved a series of processes, including smelting raw material ore and making alloys followed by various thermo-mechanical treatments. These processes were often integrated with the technological traditions reflecting temporal and regional characteristics. By the twelfth century BCE, carburization was successfully used to make knives and blades in the eastern Mediterranean. Using the quenching technique, iron was further hardened. However, at the same time, quenching made the metal brittle therefore the technique of tempering was used. By the seventh century BCE, the process of carburization and quenching was used to produce a form of iron steel which had a higher tensile strength. A harder iron could then be utilized to make better weapons and tools as compared to bronze [6]. Weapons played a major role in the battles of ancient Egypt, and some believe that these weapons developed at the beginning from the tools that the ancient Egyptian used for the purposes of daily life, and then they were modified with their function in wars, fig. (2). by looking at the ancient history, we find that the axe was used by soldiers in various shaped. In general, the axe was made through two methods. The first one was produced using segmented molds, which have a front and a back part installed on each other. The molten metal was then poured into it through the sprue. The second method is to use the mold and hammering by pouring the molten metal into the mold and then hammering the piece to get it out in the desired shape [9]. The iron axes began by copying the bronze forms; which continued until the Iron Age which began in Egypt at the eighth century B.C. In Nubia, iron was not known before the sixth century BC [10]. Axes were made from four separate components: firstly, the bulk of the axe that had been made from a rolled tube; then the steel cutting edge; then also a wedge-shaped filling in the blade; and a slag-rich filling in the socket. As the axe turned out to have undergone quite a complex forging technique [11]. The present study focuses on the analysis of an iron axe head discovered in Egyptian Nubia, employing a range of laboratory techniques. Given the limited data on the metallurgy and analytical study of steel from that civilization, it is crucial to expand the body of literature concerning ancient steel production in the region. Future studies are necessary to reveal the chemical composition and microstructure of archaeological iron artifacts, thereby shedding light on the technologies used in iron production and manufacturing during that period.

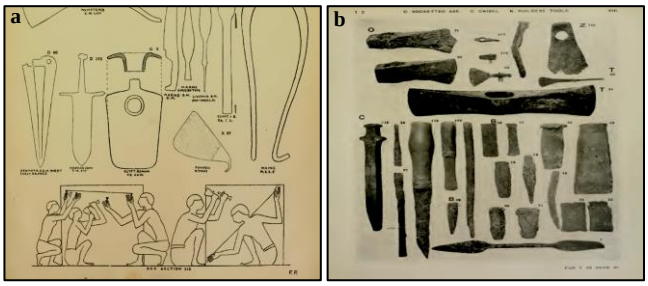

Figure (2) **a.** iron axes manufacturing process**, b.** shapes of axe head and daily life tools.

This research specifically investigates the metallurgical properties of the axe head currently housed in the Egyptian Museum in Cairo. It emphasizes the importance of examining the composition, microstructure corrosion products through microscopic, micro analytical and analytical techniques. A primary objective is to better understand the corrosion mechanisms and morphological changes in archaeological iron, particularly low-carbon steel, resulting from long-term burial. This includes analyzing the physico- chemical processes that contributed to the artifact's degradation and identifying the environmental conditions that influenced its corrosion. Moreover, the results aim to support informed decision - making in selecting appropriate conservation treatment methods for the analyzed axe head. As well as in characterizing decay mechanism in excavated iron artifacts more broadly. Finally, it also seeks to determine the most appropriate display method and materials for the axe head, ensuring its safe and meaningful redisplay following conservation.

2. Materials and Methods

2.1. *Materials*

2.1.1. Preparation of archaeological samples

Corrosion products samples were prepared by grinding into powder in an Agate mortar. Fragments of the artifact were mounted in a two-part epoxy resins mold and ground using silicon carbide papers with progressively finer grit sizes (from 1000 to 4000). The samples were polished by using diamond paste 0.25 mm, and etched with Nital Solution (2% v./v nitric acid in ethanol -100 ml ethanol and 2ml nitric acid) [10] and washed in a distilled water then dried.

2.1.2. Acidity treatment solution (Desalination)

Alkaline Sulfite Treatment solution (0.1M wt./v sodium hydroxide 4g/l + 0.05M wt. /v alkaline sodium sulfite 6.3g/l) was selected for the removal and extraction of chlorides [12].

2.1.3. Polypropylene acid free plastic

A temporary preservation process was carried out by using a sealed polypropylene acid free plastic box to protect and insulate the axe head from the surrounding environmental conditions [13].

2.1.4. Poly (methyl methacrylate)

Known as Plexiglas, Perspex, Acrylate or simply acrylic, was used for redisplaying the axe head.

2.2. *Methods*

Different investigation and analytical methods were applied for identifying and characterizing both metal core and deterioration phenomena as follow:

2.2.1. Portable digital light microscope (USB)

For the investigation, surface inspection of the axe head, and to follow up the various treatment stages, a portable digital light microscope (USB) model Dino capture 2.0 version 1.5. 12, 2013, Armo electronics corporation at the conservation department of the Egyptian Museum was used.

2.2.2. Stereo microscope

Stereo Microscope model Toup-cam T4, X Cam HD Camera LEICA6, made in Germany, (80x), at the Metals Research and Development center, Helwan, was used to examine the various colors of corrosion products.

2.2.3. Metallographic microscope

Investigation of metal core was performed using metallographic examination using Metallography-Zeiss with Software: AXIOVISION, optical microscope at the Metals Research and Development center, Helwan. was used to examine the various colors of corrosion products.

2.2.4. SEM-EDX investigation and analysis

Scanning electron microscope coupled with energy dispersive x-ray spectroscopy (SEM-EDX) was used. Device model Quanta, FEG250 FEI TM, Quanta FEG250 scanning electron microscope (FEI Company, Hillsboro, Oregon-USA), voltage of 20 KV., at the Desert Research and Development center in El-Matarya-Cairo.

2.2.5. X-ray Diffraction Analysis

X-Ray diffraction analysis, Smart Lab Rigaku, coupled with a hyper- 3000, high -energy- resolution 2D, multidimensional semiconductor detector, (Japan), at the Electronics Research institute, El-Nozha, Cairo.

2.2.6. Portable X-ray Fluorescence (p-XRF)

XG LAB (BRESCIANI S.R.I.) (France), at the Egyptian museum conservation department in Cairo.

2.2.7. Raman Spectroscopy

Samples were analyzed using BRUKER SENTERRA II Model 2019 .20x, Laser 785 nm, Power10 nm, model 2019, at the Antiquities Research and Conservation Center - Projects Sector - Ministry of Tourism and Antiquities.

2.2.8. FTIR Spectroscopy

Fourier transform infra-red spectroscopy, model JASCO, FTIR-460, (Japan), at the Micro Analytical Center, Faculty of Science, Cairo University.

3. Results

3.1. *Descriptions and visual investigation*

The study focuses on an archaeological iron axe head from Nubia (Ballana and Qustul), displayed at the Egyptian Museum in Cairo (No.70753). The axe head is approximately (L. 25x W. 18 cm). The thickness clearly increased and varied from area to another, but the average thickness is (1.3 cm), fig. (3-a). The axe head was documented using photographic documentation, fig. (3-b).

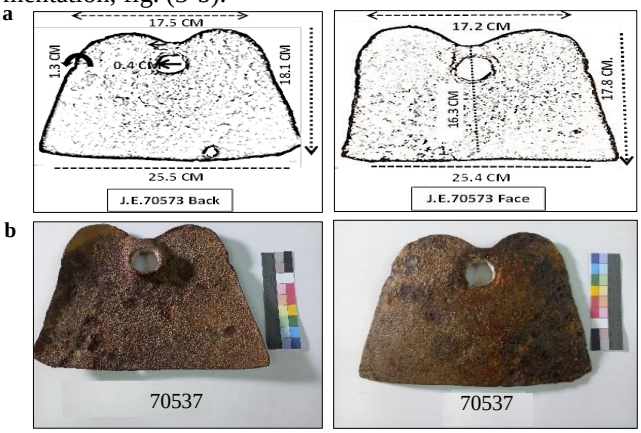

Figure (3) **a.** the iron axe head dimensions (Length& width& thickness), **b.** photographic documentation of the axe head object from the back and the front.

3.2. *Characterization and condition assessment of the iron axe head*

Visual and microscopic examination of the axe head reveal that it has undergone extensive corrosion and was heavily deteriorated. The object is entirely covered with a thick crust of corrosion products, displaying rust compounds in various colors - red, yellow, brown, black and orange - across large portions of the surface. This variation in color and extent of corrosion indicates multiple stages of damage, along with the transformation of substantial areas of the metal object [10]. Several distinct deterioration features were detected, including weeping iron phenomena, large accumulations of rust intermixed with soil deposits, noticeable thickening of the axe head due to the buildup of corrosion layers, the complete loss of the wooden handle, a general decline in the mechanical and physical properties resulting in weakened cohesion due to microstructural defects [12], and a missing area in the body of the object. The rough outer rust layer exhibits swelling, exfoliation, flaking, erosion and pitting. These deterioration features collectively indicate the probable aggressive and corrosive burial environment. The metallic core of the axe head has suffered substantial material loss, making it extremely fragile and brittle, fig. (4). Additionally, a white, glossy coating layer was observed on the surface. Based on its appearance and texture, this coating may be a protective layer applied during previous conservation intervention. Overall, the condition of the object is unstable, with widespread corrosion and compromised structural integrity. Referring to deterioration factors [14]. It can be derived that the rust crust likely formed as a result of either the burial environment or inadequate storage or display conditions. However, comparative studies of objects excavated from the same cemetery support the former explanation. These studies confirm that similar degradation patterns were present in other artifacts, suggesting that the burial environment was the primary contributor to the current condition of the axe head [10].

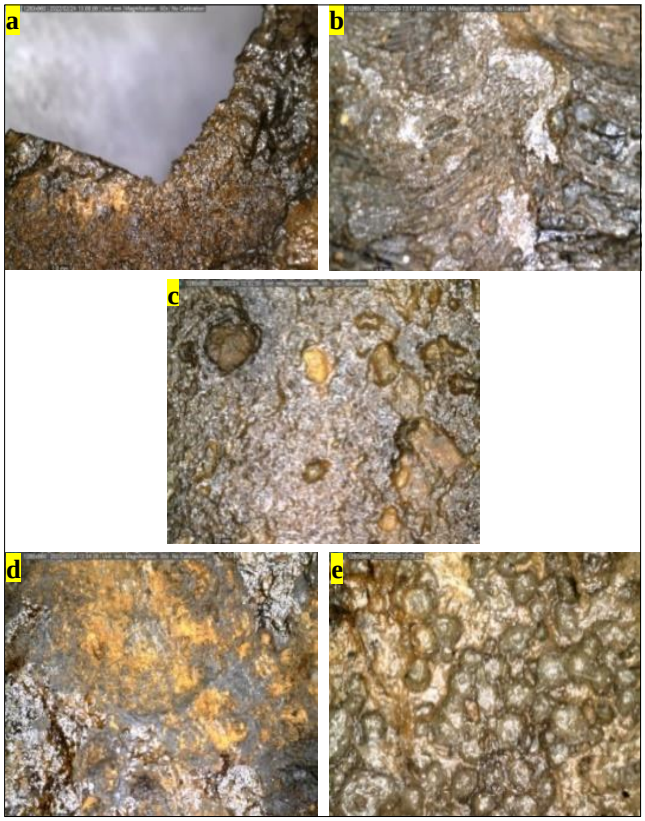

Figure (4) portable light microscope images (40-x) showing different corrosion phenomena **a.** losses and holes, **b** different soil deposit, **c.** erosion of object surface, **d.** orange corrosion an indication of active corrosion (akageneite) as confirmed by XRD analysis, **e.** formation of goethite (iron oxide hydroxide).

3.3. *Stereo microscope results*

Examination of the corroded surface of the axe head under a stereomicroscope revealed the presence of different corrosion layers. A reddish-brown corrosion layer was identified, which corresponds to the typical formation of goethite (α-FeOOH), a common corrosion product in iron artifacts was observed [10, 15]. Some areas of the artifact displayed visible deterioration, including cracking, splitting and flaking, particularly on broken sections. This could be attributed to volume expansion caused by the formation of goethite [16]. Additionally, the presence of yellow - brown corrosion products indicate the formation of lepidocrocite (γ- FeOOH) as confirmed by X-ray diffraction XRD analysis [17,18]. Active corrosion was observed over large areas of the axe head surface, marked by the presence of akageneite (β-FeO (OH)), commonly associated with the "weeping iron" phenomenon, fig. (5-a. & b.). A black corrosion product, identified as (Magnetite Fe_3O_4), was also detected and confirmed by XRD analysis, fig. (5-c). Under low magnification, additional microscopic features were noted, such as deep cracks and shiny blisters, likely resulting from ongoing corrosion process, including weeping [19]. Across many areas of the object, various forms of damage were evident, including cracks, flacking, dust deposits, holes, material loss, erosion and weeping. Furthermore, the outer metallic layers have largely transformed into corrosion products, fig. (5-d).

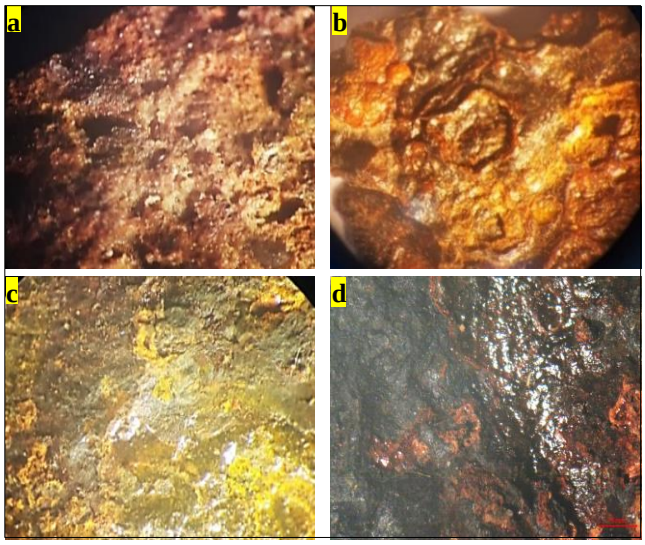

Figure (5) stereo microscope examination of iron axe head samples with Various magnification power. It shows multiple signs of damage and rust formation with different colors (yellow- orange- brown- red- black) **a.** & **b.** weeping iron phenomenon (80-x), **c.** the formation of goethite and lepidocrocite (50-x), **d.** black magnetite, cracks and flacking (60-x) black magnetite, cracks and flacking (60-x).

3.4. *Metallographic results*

The investigation of the corrosion layer and metallic structure were conducted on the samples of the polished cross-section before and after etching [10]. The alloy composition of the axe head was determined through metallographic examination. It revealed that the metallic matrix of the axe head was manufactured from low-carbon steel (hypoeutectoid steel), a type of steel characterized by a relatively low carbon content [15]. The microstructure of this steel is primarily composed of ferrite and pearlite phases, which were clearly distinguished in the metallographic plates, figs. (6-a, b & c). Based on the observed microstructural features, it was deduced that the axe head was manufactured using the hot forging technique [20].

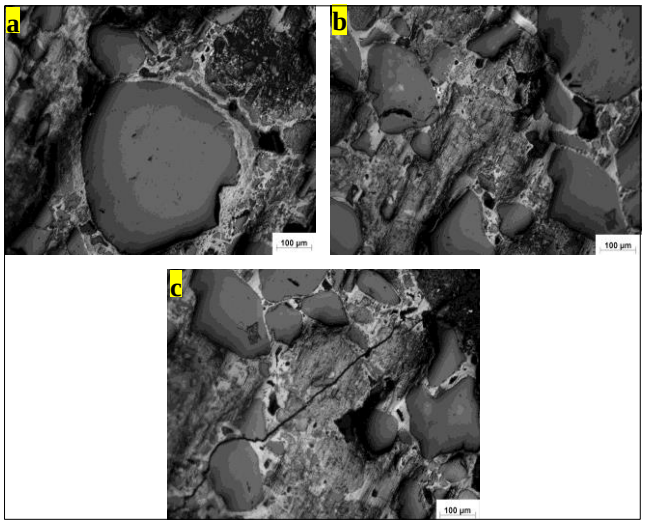

Figure (6) metallographic examination of etched samples from the axe head; **a. & b.** demonstrate the micro structure of pearlite, **c.** ferrite grains featured for low carbon steel, manufacturing method by hot forging

3.5. *SEM results*

Scanning electron microscope (SEM) images, taken before and after etching of the samples, revealed the presence of active rust and formations of iron oxides, fig. (7-a). Rust compounds appeared interspersed with cracks and separations, fig. (7-b) likely formed due to prolonged exposure to the burial environment [10]. Moreover, cracks and micro cracks of variable sizes and shapes were clearly evident on the surface and between the crystalline structures. These features indicate significant deterioration of the metal's mechanical and physical properties, resulting from the development of these cracks and the accumulation of rust layers, as observed both in SEM images, fig. (7-c) and through visual examination. Microscopic observations revealed that the corrosion layers on the axe head are consistent with the corrosion morphologies typically observed in iron artifacts buried in soil environments. This suggests that the object is highly vulnerable to further corrosion and deterioration under unsuitable environmental conditions [20]. SEM investigation also revealed the presence of soil minerals and goethite within the microstructure. In some areas, the surface was found to be heavily enriched with soil minerals than with goethite corrosion products. One of the most notable forms of deterioration observed is the weeping phenomenon, which refers to the appearance of hollow, bead-like structures on the corroded surfaces of excavated iron artefacts. This type of corrosion is indicative of progressive deterioration caused by chloride contamination, which promotes active rusting after excavation [16,21].

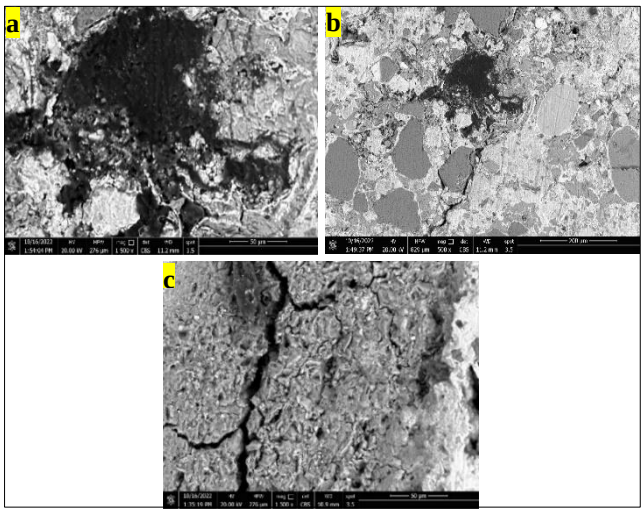

Figure (7) SEM micrographs of the axe head; **a.** notice rust areas of iron oxides (1500-x) in addition to the slag inclusions, **b.** micro and various cracks and separations with an overlap between the layers of rust and sand grains in many areas (800-x), **c.** different shapes of cracks "micro and wide" (1800-x).

3.6. *Elemental analysis results*

Portable X-ray fluorescence (PXRF) was used to study the elemental composition of the object's metal core, slag inclusions and corrosion layers [15,22]. The analysis confirmed the significant presence of iron as the main alloying element, with the presence of other constituents such as silicon (Si), calcium (Ca), and chlorine (Cl), in addition to other trace elements as lead (Pb), copper (Cu), and zinc (Zn). Six spots were analyzed using PXRF: spots 1 to 3 were taken from the metallic core and are shown in tab. (1) and fig. (8), while spots 4 to 6 were taken from the external corrosion, tab. (2) and fig. (9). A high percentage of calcium was recorded in tab. (1) and tab. (2), which may be attributed to the use of limestone (calcite) as a flux during the ancient extraction process. Calcium oxide (CaO) is known to increase the basicity and decrease the viscosity of liquid slag, which aids the separation of iron from slag and enhances the yield of extracted iron [23]. The presence of slag in ancient iron is not only due to the composition of the ore used but is also influenced by the smelting system used in ancient furnaces. These systems often involved fuel ash, fluxes and furnace linings, as is often noted in recent literature and studies on historical metallurgy [24]. The analysis also revealed a notably high concentration of silicon at several points, tab. (2). This may be related to the presence of quartz (SiO_2), which was observed on the surface of the artifact. The presence of quartz is likely a result of the burial in a soil-rich environment and was clearly identified through microscopic examination using SEM and stereomicroscopy (SM), figs. (5 & 7). These quartz particles were found deeply embedded in the corrosion layers and firmly adhered to the artifact, making them difficult to remove. The grains were distinctly visible under microscopic examination, fig. (7) [10], and their presence was further confirmed using XRD analysis. Chloride contamination of the artifact was evident from the elemental analysis presented in tabs. (1 & 2). This indicates the diffusion of chlorine ions and their compounds into the artifact as a result of the reactions with soil anions, which has significantly contributed to its deterioration. The progression of corrosion caused by chloride is further supported by the observed 'weeping' phenomenon. This form of active corrosion is associated with the presence of akageneite (ß FeOOH), which was identified and confirmed using XRD.

Table. (1) PXRF elemental analysis results of the metallic core.

NO.	Fe	Ca	Zn	Cu	Cl	Pb
1	66.21	11.97	0.78	-	16.55	4.5
2	72.5	24.93	0.57	1.14	-	0.86
3	81.07	14.88	-	-	-	4.05

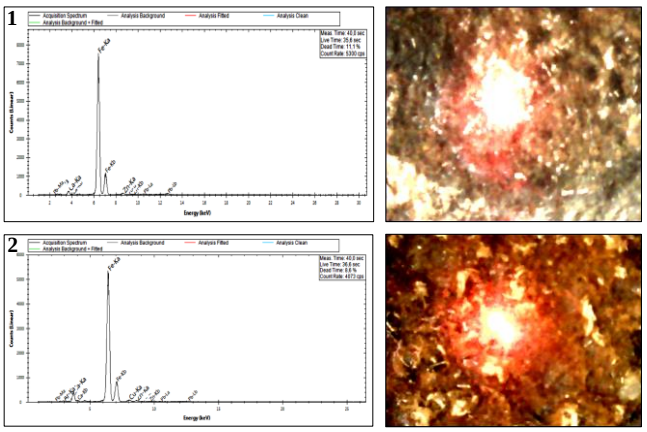

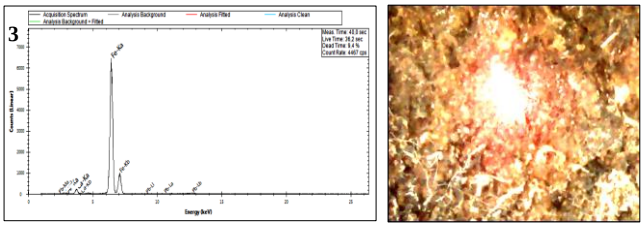

Figure (8) PXRF patterns of spots analysis (1:3) of the *metallic core parts* of the axe head revealed the percentage of Fe in high concentration as the main element.

Table (2) PXRF elemental analysis results of the corroded parts.

NO	Fe	Si	Ca	Zn	Cu	Cl	Pb
4	4.75	26.79	67.83	0.65	-	-	0.16
5	5.96	51.44	36.09	0.52	0.44	4.89	0.66
6	43.03	-	48.46	1.21	-	6.06	0.73

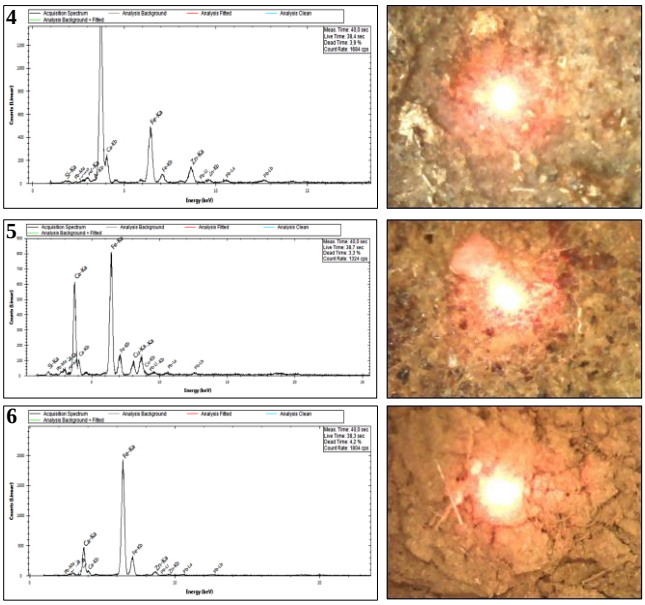

Figure (9) pXRF results from spots 4 and 6 on the corroded axe head, indicating high Fe content, significant Cl, responsible for weeping iron, was detected, along with variable Si and minor Al and Na contamination.

3.7. *XRD analytical results*

Three samples of the rust layers were analyzed and revealed the presence of magnetite (black), goethite (red brown), lepidocrocite (yellow-brown) in some areas, and akageneite (orange), tab. (3). Moreover, the analysis identified the presence of quartz (SiO_2), fig. (10) as a result of burial in soil [10]. This also explains the high silicon content on the corroded iron surface, as observed in the elemental analysis conducted by PXRF, figs. (8 & 9). Magnetite (Fe_3O_4), goethite (α-FeOOH) and lepidocrocite (γ-FeOOH) are corrosion products typically formed under specific environmental conditions. The mechanism of formation of these products can be explained as follows: at the beginning of the corrosion process, due to high aeration of the burial soil, mainly magnetite forms. Over time, with prolonged burial and continuous reactions, the magnetite layer increases in thickness and may develop cracks parallel to the metal/magnetite interface [25]. The burial environment, being close to the river Nile, suggests that the soil is saturated with water. As a result, the magnetite layer, in contact with water saturated soil, allows water to penetrate the cracks. In the presence of water, iron continues to the oxidize to Fe^{2+}.Two hypotheses arise from this process; either the magnetite layer continues to grow, or other phases such as lepidocrocite and maghemite (a common transformation product of magnetite) begin to form, tab. (3). Previous studies have indicated that magnetite can transform into maghemite or lepidocrocite [20]. Akageneite likely formed due to the presence of chlorine in the soil water [10]. Raman Spectroscopy further confirmed the rust products identified by XRD.

Table (3) X-ray diffraction analytical results

Analysis area	Chemical composition	Phase
Orange	β-Feo (OH)	Akageneite
Reddish brown	α-Feo OH	Goethite
Black	Fe_3O_4	Magnetite
White–yellow.	SiO_2	Quartz
yellow-brown	γ- Feo (OH)	Lepidocrocite

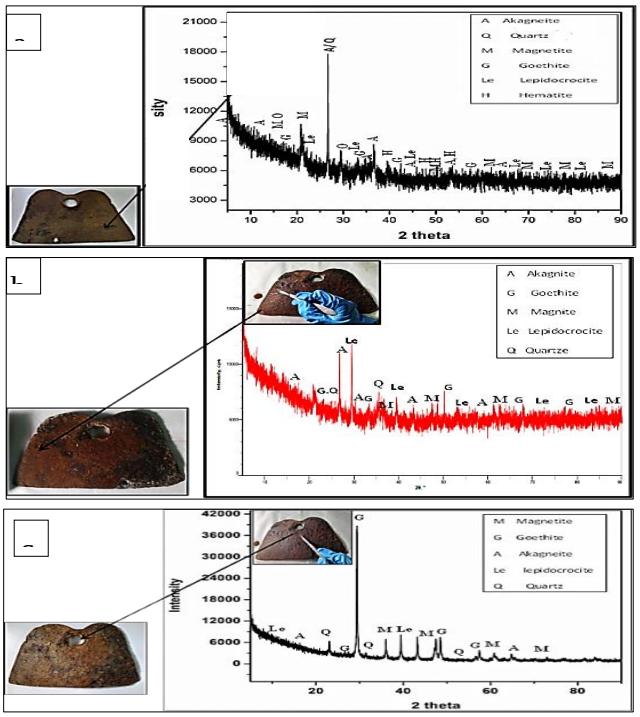

Figure (10) XRD patterns of corroded samples revealed that the defined products are (magnetite, lepidocrocite, goethite, akageneite and quartz).

3.8. *Raman spectroscopy analytical results*

Raman spectroscopy confirmed the corrosion products previously identified by XRD, fig. (10). These corrosion products were identified using micro-Raman analysis before etching; which is important because etching can alter the chemical composition of the corrosion products [26]. The thickness of the rust layer is also strongly influenced by the corrosiveness of the burial environment including factors such as pH, aeration and the presence of soluble salts [10]. Raman spectral analysis of the corrosion samples showed that the orange corrosion products were identified as akaganeite (β- FeOOH), characterized by identifiable bands at 726, 538, 413, 387, 299 and 139 cm^{-1} [21], fig. (11-a). The yellowish corrosion areas disp-

layed a sharp, intense band at 666 cm^{-1}, with additional peaks at 300 cm^{-1}, and peak at 890 cm^{-1}, fig. (11-b). These three bands are characteristic of magnetite (Fe_3O_4) [22]. Although magnetite (Fe_3O_4) is intrinsically black, its detection within visually yellowish corrosion areas can be explained by the heterogeneous nature of archaeological corrosion layers. Raman spectroscopy, owing to its high spatial resolution, is capable of detecting magnetite locally even when it does not dominate the macroscopic appearance of the corrosion layer. Moreover, the red corrosion products analyzed at the same spot, showed Raman peaks at 222, 292, 406, 607, 1318 and 1592 cm^{-1} [44], fig. (11-b), indicating the presence of Hematite phase (α-Fe_2O_3. (These corrosion products were mixed with yellow-brown corrosion products identified as lepidocrocite (γ-FeOOH), detected as a large band at 378 cm^{-1} and various medium bands (139, 248 and 1312 cm^{-1}) [21], fig. (11-c). In addition to the dark reddish brown corrosion products which displayed peaks at 241, 299, 378, 480, 549 and 646 cm^{-1}, fig. (11-c) indicating the presence of goethite (α- Fe-OOH) [9]. The identified corrosion phases are summarized in Tab. (4). These findings suggest that the rust compounds formed as a result of reactions with soil anions, including dissolved sulfate and chloride ions, contributing to the corrosion of the iron artifact [27].

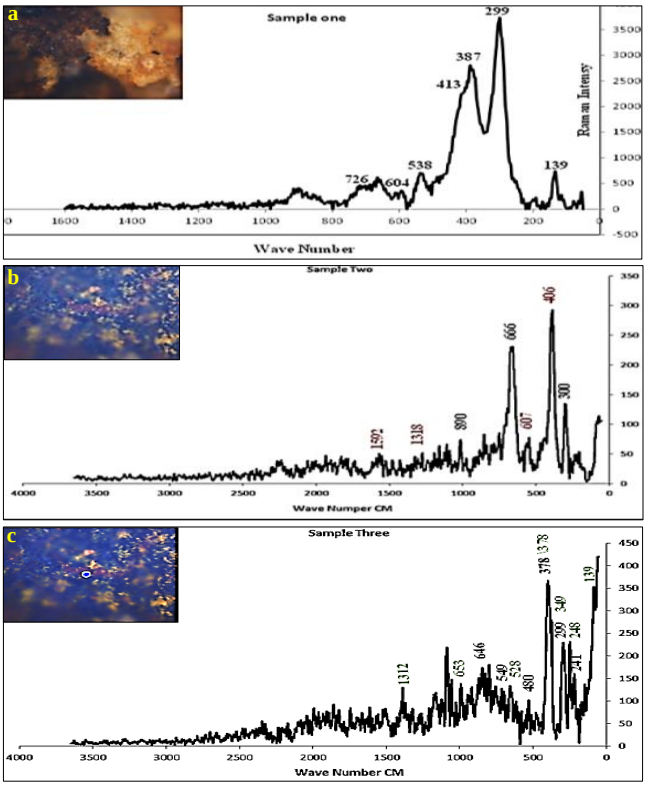

Figure (11) Raman spectra patterns of corrosion products, **a.** akaganeite, **b.** magnetite and hematite, **c.** lepidocrocite and goethite.

Table (4) results of the Raman spectroscopy analysis of rust samples

Color	Raman peaks CM	Phase	Chemical formula
Dark Reddish brown	241-299-378-480-549-646	Goethite	α- Fe-OOH
Black	300-666-890	Magnetite	Fe_3O_4
Orange	139-299-387-413-538-604-726	Akageneite	β-Feo (OH)
yellow-brown	248-301-349-378-1312-139-528-653	Lepidocrocite	γ- Feo (OH)
Red-Brown	222-292-406-607-1318-1592	Hematite	α-Fe_2O_3

3.9 *FTIR analytical results*

The study revealed the presence of previous restoration materials, including a coating layer on the surface of the artifact, which was identified using FTIR analysis [10]. The results were compared with the FTIR spectra of standard reference samples [28], revealing that the coating consisted of a mixture of acrylic resin, beeswax and paraffin wax, this combination was previously applied as a protective coating layer, fig. (12). In the figure, "A" corresponds to the acrylic standard, "B" to the beeswax standard, "P" to the paraffin wax standard and "S" represents the archaeological coating sample spectrum. The results of the analysis are listed in tab. (5).

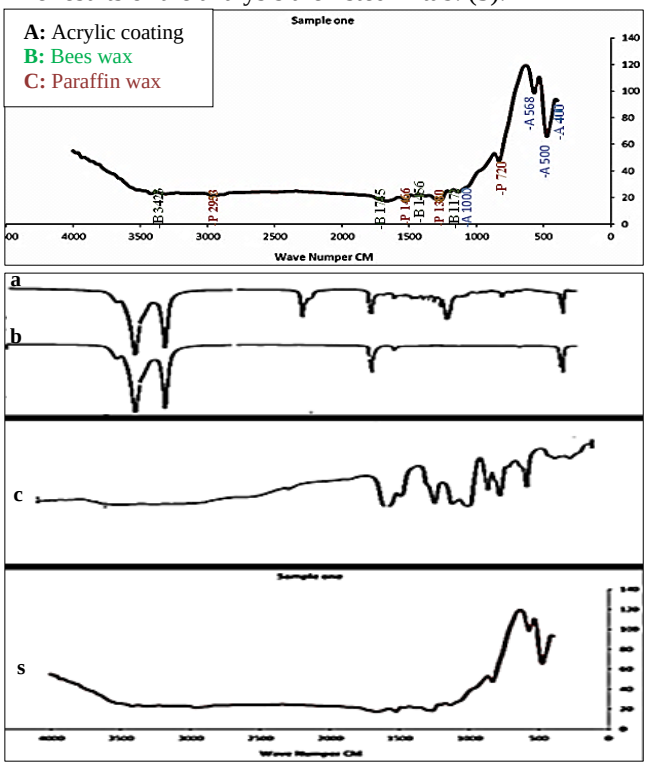

Figure (12) FTIR analytical results of the ancient protective coating were consistent with the FTIR spectrum, **a.** beeswax standard spectra, **b.** paraffin wax standard spectra, **c.** acrylic standard spectra, **s.** archaeological coating sample.

Table (5) results of FTIR analyses of a protective coating sample. components

Identified Compound	Wave No in CM	Functional Group
Acrylic	400- 500- 1000 CM	833 CM, C-O bending bond. 1263 CM, C-O bending bond. 1467 CM, C-H bending bond. 1666 CM, C-O Stretching bond. 2965 CM, C-H Stretching bond.
Paraffin Wax.	720- 1380-1466-2847-2910 CM	1196 CM, C-O Stretching bond. 1467 CM. C-H bending bond.
Bees Wax.	1163-1456- 1720 CM	1163 CM, C-O Stretching bond. 1172CM, C-H tending vibration. 1456 CM, C-C Stretching. 3311, 3423 CM, OH week [27].

4. Discussion

The examination of the archaeological axe head using various analytical techniques revealed that the artifact was made of low-carbon steel, as the presence of both pearlite and ferrite phases was observed in the metallographic analysis, fig. (6) [9]. Visual investigation revealed the presence of different det-

erioration features, including material loss, active corrosion, surface cracks, mechanical and structural weakness, and the weeping phenomenon. It was concluded that the burial environment played a significant role in the degradation of the object. The soil in which the artifact was found was likely saturated with water due to its proximity to the river Nile, creating conditions that promote constant exposure to moisture [5]. X-ray diffraction and Raman spectroscopy analyses of the corrosion layers confirmed the presence of several corrosion products, including akageneite, goethite, magnetite, and lepidocrocite, figs. (10 & 11). Akageneite formation indicates the presence of chloride-rich conditions in the burial soil [22], while magnetite forms under well-aerated environments. Over time, as corrosion processes continue, magnetite layers increase in thickness, and internal stresses may lead to the formation of parallel cracks. These cracks allow further moisture penetration, facilitating the development of secondary corrosion products such as lipidocrocite and maghemite [26]. The overall findings indicate that the artifact is in an unstable state and undergoing active corrosion. Accordingly, a series of appropriate conservation measures were implemented. Mechanical cleaning was carried out to remove surface dirt and thick rust layers, revealing the original surface morphology. A portable digital microscope was used throughout the process to closely monitor progress. Given the widespread presence of pitting and active corrosion, especially the weeping phenomenon, local desalination using an alkaline sulfite solution proved effective in stabilizing the object and mitigating further chloride-induced deterioration [29]. Due to the fragile condition of the axe head, conservation and restoration procedures extended over several weeks. Temporary protective measures were applied within the conservation laboratory to ensure a controlled microenvironment. This included the use of a tightly sealed, acid-free container and a moisture-absorbing material to maintain a stable RH below 15 % [12]. Furthermore, because of the weakened mechanical properties and the presence of active corrosion, the application of a corrosion inhibitor (tannic acid) followed by a protective coating (Paraloid B-72) was essential. These layers served to stabilize the surface, protect it from environmental exposure, and improve its durability and appearance [9]. Upon completion of the restoration, preventive conservation strategies were implemented. A new display system was designed to replace the previous method, which had directly exposed the axe head to damaging materials such as wood and textile, and placed it in contact with adjacent iron artifacts, increasing the risk of galvanic corrosion. A custom mount was fabricated to securely support and display the axe head without physical stress or chemical interaction [12,13].

5. Conservation Process

Based on the previous results and above mention data, we could achieve the following conservation procedures:

5.1. *Temporary preservation process*

A temporary preservation process was carried out during the conservation stages of the iron axe head [30]. The object was stored in a sealed polypropylene acid free airtight plastic box to protect it from external environmental conditions [31]. Indicating silica gel was added inside the box to maintain a RH level below 15 % helping to preserve the corroded iron. The silica gel should be monitored and replaced every 3 months to ensure its continued effectiveness [10]. Additionally, an acid free support and tray was prepared to allow for the safe and appropriate handling of the object. For further protection, the axe head was wrapped using cushions made from Japanese paper and packing cotton [13], fig. (13).

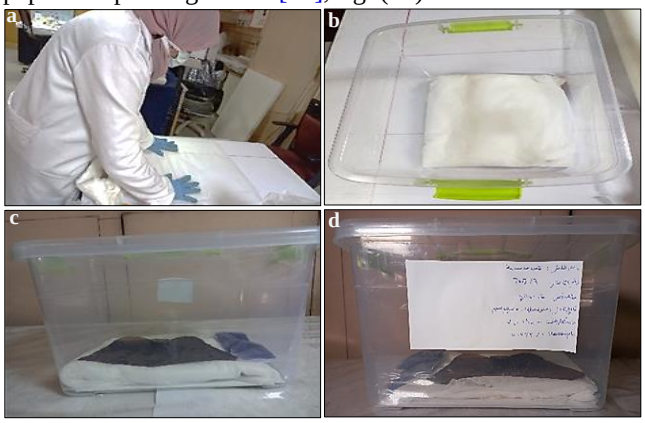

Figure (13) the iron axe head temporary preservation; **a.** preparing a cushion, **b.** put the cushion inside a polypropylene box. **c.** put the object in a box with indicating silica gel, **d.** sealed the box and bring a label contain enough information about the object and date of preservation process.

5.2. *Cleaning process*

Based on the analysis of corrosion compounds, figs. (10 & 11) and the detailed examination of the artifact, it was determined that the iron axe head was affected by active corrosion, characterized by a thick corrosion crust, figs. (4, 5 & 7), along with surface dirt and remnants of burial soil, fig. (7). Therefore, a surface treatment was necessary to stabilize the object and improve its condition [32]. The cleaning process included the following stages: **1st stage:** The initial step aimed to improve the surface appearance by removing thick deposits from the corroded surface through mechanical cleaning [12]. This was done using soft brushes of various sizes to carefully eliminate corrosion compounds, dislodged soil particles, and dust deposits without damaging the underlying metal [10], fig. (14-a). **Second stage:** Surface rust and soil concretions were further reduced using more precise mechanical tools such as toothbrushes, a micro motor, fiberglass pens, and scalpels to remove the thicker corrosion layers [33], fig. (14-b). After completing the mechanical cleaning, the artifact was examined under a microscope to assess the results and identify any remaining corrosion or damage, fig. (14-c & d).

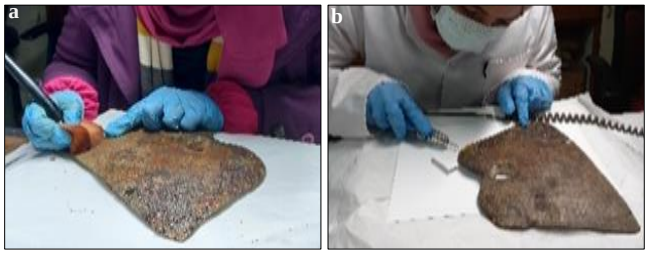

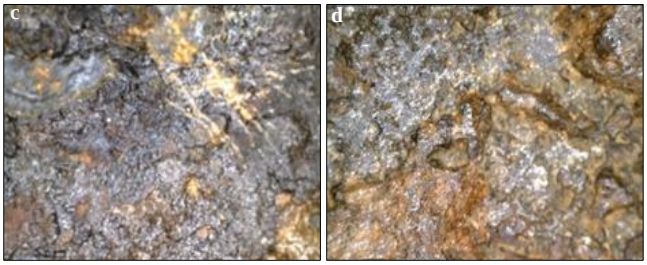

Figure (14) mechanical cleaning processes of the iron axe head using **a.** soft brushes for removing loose soil, **b.** micro motor to reduce rust thickness, **c.** & **d.** microscopic images after mechanical cleaning.

3rd Stage: Due to the fragile condition of the axe head, the presence of cracks, and the detection of the weeping phenomenon—confirmed by XRD and Raman spectroscopy, fig. (10 & 11) as well as microscopic investigations, fig. (5-7) which revealed the presence of akageneite (β-FeOOH), an active corrosion product, a chemical cleaning process through desalination was selected. This process aimed to remove chlorides from the axe head using an alkaline sulfite treatment, consisting of sodium hydroxide and alkaline sodium sulfite [34]. The treatment solution was prepared using 4 g/L NaOH and 6.3 g/L Na_2SO_3, fig. (15-a). This method was chosen to enhance the stability of the object and to reduce surface acidity. The progress of the treatment was closely monitored under microscopic examination to ensure the effective removal of chlorides without altering the shape or structure of the object, fig. (15-b). After the desalination process was completed, the axe head was rinsed several times with distilled water to remove any remaining chemical residues. Finally, the object was dried using alcohol [35]. The entire cleaning process was documented photographically before, during, and after treatment, fig. (15-c & d).

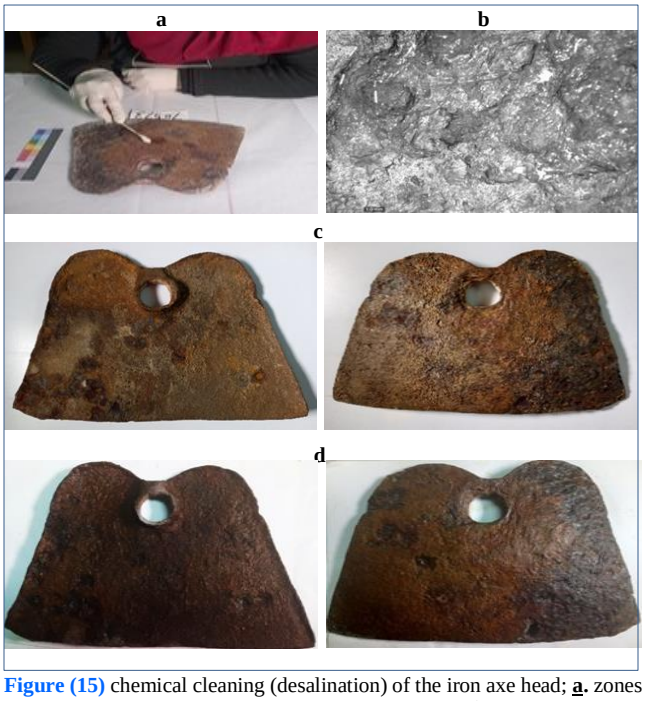

Figure (15) chemical cleaning (desalination) of the iron axe head; **a.** zones with active rust, **b.** microscopic image after cleaning, **c.** the axe before treatment, **d.** after treatment (60-x)

5.3. *Stabilization and applying of protective Coating*

Corrosion inhibition was carried out using a 5% wt./v solution of tannic acid in acetone, applied to the surface by brushing [32]. Tannic acid is a natural, non-toxic, and environmentally friendly corrosion inhibitor. Its protective effect is attributed to the formation of a stable ferric tannate film on the surface of the steel, which remains relatively durable even under humid conditions. This process was carried out to protect the object from future corrosion and to achieve surface stability [25]. The tannic acid layer acts as a physical barrier, preventing the penetration of corrosive agents to the base metal [36]. Additionally, it enhances resistance to environmental factors such as weathering, relative humidity, and friction, while also contributing to the durability and visual appearance of the artifact. Several layers were applied to achieve a uniform and consistent finish [21]. Given that completely or partially mineralized iron artifacts typically suffer from microstructural weakness, cracks, and a loss of many original metallic properties, a protective coating was applied following the inhibitor treatment. Once the tannic acid layer was fully dried, a 5% wt./v solution of Paraloid B-72 in toluene was applied by brushing. This coating serves to prevent the formation of new corrosion products, improve the mechanical strength and surface stability of the axe head, and consolidate the object for safe display, particularly due to its fragile condition [33]. Both the inhibitor and the protective coating were selected for their availability, proven effectiveness, and reversibility [32], fig. (16).

Figure (16) applying stabilization and protective coating

5.4. *Redisplaying of the axe head*

An improved redisplay plan was developed and implemented, as the previous display method had contributed to the deterioration and corrosion of the object [33]. The axe head had been in direct contact with the materials of the display case, which likely accelerated corrosion. Additionally, it was positioned adjacent to other iron objects, increasing the risk of galvanic corrosion due to the close proximity of dissimilar metals [31]. The original display angle and height were also found to be unsuitable, making it difficult for visitors to view the object comfortably. To address these issues, a custom Plexiglas display holder and stand were designed and fabricated with appropriate dimensions and height to accommodate both the object and the existing display case [30]. This ensured a secure and stable presentation of the iron axe head. The stages of preparing the new display stand and the final installation of the artifact are shown in fig. (17).

Figure (17) the object after re-displaying on plexiglass stand.

6. Conclusion

The iron axe head analyzed in this study was excavated from the Ancient Egyptian Nubian sites of Ballana and Qustul. Its burial in aerated sandy soil led to significant chemical, structural, and morphological deterioration. The object is now extremely fragile due to an extensive corrosion process that formed a thick rust layer. Compositional analysis identified the metal as low-carbon (hypoeutectoid) steel. Analytical techniques, including SEM and XRD, confirmed the presence of corrosion products such as magnetite, goethite, lepidocrocite, and akageneite. The appearance of the "weeping" phenomenon signals ongoing active corrosion. Stereo microscopy showed colored corrosion products mixed with soil minerals like quartz and calcite. These findings point to a moisture-rich burial environment that accelerated corrosion. Conservation measures focused on chloride removal and stabilization using an alkaline sulfite desalination treatment. Tannic acid in acetone was applied as a corrosion inhibitor, followed by a protective Paraloid B-72 coating, applied by brush to safeguard the object from future deterioration. Finally, the axe head was then safely mounted for redisplay. This study highlights how scientific analysis supports effective conservation strategies for fragile archaeological iron artifacts.

Acknowledgements

The authors would like to thank Prof. Dr Mohamed Abd- EL Rahman, Professor of Metallography, National Institute of Metals Research, and special thanks go to Egyptian Museum-Conservation department, for their support and help in this work, a considerable and great thanks to the editors of the journal for through reviewing and editing.

References

[1] Williams, B. (1991). *Excavations between Abu Simbel and the Sudan frontier, Part 8: Meroitic remains from Qustul cemetery Q, Ballana cemetery B, and a Ballana settlement*, The University of Chicago Oriental Institute Nubian Expedition, USA.

[2] Dann, R. (2009). *The archaeology of late antique Sudan: aesthetics and identity in the royal X-group tombs at Qustul and Ballana*, Cambria Press, Amherst.

[3] Location map of ancient Nubia, Ballana and Qustul., *www.touregypt.net* (25/2/2024).

[4] Walter, E. (1983). *The royal tombs of Ballana and Qustul*, Vol. I. Cairo Government Press, Cairo.

[5] Dann, R. (2007). *Aesthetics and identify at Qustul and Ballana lower Nubia*, PH.D., Archaeology dept., of Durham Univ., England

[6] Elaref, M. (2020). Iron ores of Egypt, Ch. 14.1. In: Hamimi, Z., El-Barkooky, A., Frías, J-M., et al. (eds.) *The Geology of Egypt*, Springer Nature, Switzerland, pp. 522-527.

[7] Williams, B. (1991). *Excavation between Abu Simbel and the Sudan frontier*. V IX. Chicago Univ., Chicago.

[8] Comilli, D., Dorzio, M., Folco. L., et al. (2016). The meteoritic origin of Tutankhamen's iron dagger blade. *Meteoritics & Planetary Sciences*. 51 (7): 1301-1309.

[9] Elashery, N., Megahed, M., El-Shamy, A., et al. (2023). Archaeometry characterization of bronze patina on archaeological axe head in military museum, Cairo. *J. of Archaeology Tourism-Must*. 2 (1): 23-33.

[10] Salem, Y., Oudbashi, O. & Eid, D. (2019). Characterization of the microstructural features and the rust layers of an archaeological iron sword in the Egyptian Museum in Cairo (380-500 A.D.). *Heritage Science*. 7, doi: 10.1186/s40494-019-0261-2.

[11] Saage, R., Kiilmann. K. & Tvauri, A. (2018). Manufacture technology of socketed iron axes, *Estonian J. of Archaeology*. 22 (1): 51-65

[12] Zidan, Y., El Hadidi, N., Mansour, M., et al. (2013). Treatment and restoration of antique sword from Ottoman period (13^{th} AH /19^{th} AD century) at the National Military Museum - Saladin Citadel in Egypt, In: VALMAR (ed.) *6^{th} Int. Cong. "Science and Technology for the Safeguard of Cultural Heritage in the Mediterranean Basin-Athens"*, pp. Centro Copie l'Istantanea, Roma, pp. 391-396.

[13] Tétreault, J. (2021). Products used in preventive conservation. *CCI Technical Bulletins.* 32: 1-71.

[14] Nordgren. E. (2016). *The effect of metallurgical structure on the chloride-induced corrosion of archaeological wrought iron*, PH.D., Schools of History, Archaeology and Religion, Cardiff Univ., UK.

[15] Srivastava, N., Singh, A, Kanungo. A., et al. (2023). *Comparative microstructural and elemental analysis of iron artifacts from Kaveri valley archaeological sites*, Ministry of Mines, India.

[16] Wang. Q. (2007). An investigation of deterioration of archaeological iron. *Studies in Conservation*. 52 (2): 125-134.

[17] Faltermeier, R. (1995). *The evaluation of corrosion inhibitors for application to copper and copper alloy archaeological artifacts*, PH.D., Conservation and Museum Studies dept., Institute of Archaeology, University of London

[18] Patel, A. (2014). Conservation of archaeological metal artifacts emphasizing on copper/bronze, *Heritage: J. of Multidisciplinary Studies in Archaeology*. 2: 347-358.

[19] Scott, D. & Eggert, G. (2009). *Iron and steel in art: corrosion, colorants, conservation*, Archetype, London.

[20] Portillo, H., Zuluaga, M., Ortega, L., et al. (2018). XRD, SEM/EDX and micro-Raman spectroscopy for mineralogical and chemical characterization of iron slags from the Roman archaeological site of Forua (Biscay, North Spain), *Microchemical J*. 138: 246-254.

[21] Pingitore, G., Cerchiara, T., Chidichimo, G., et al. (2014). Structural characterization of corrosion product layers on archaeological iron artifacts from Vigna Nuova, Crotone (Italy), *J. of Cultural Heritage*. 16 (3): 372-376

[22] Neff, D., Dillmann, P., Descotes, M., et al. (2006). Corrosion of iron archaeological artifacts in soil: Estimation of the average corrosion rates involving analytical techniques and thermodynamic calculations. *Corrosion Science*. 48 (10): 2947-2970.

[23] Kostova,B., Paneva, D., Zheleva, Z., et al. (2023). Ancient metallurgical iron slages-chemical, powder x-ray diffraction and mossbauer spectroscopic study, *Crystals*. 13 (6), doi: 10.3390/cryst13060888.

[24] Buchwald, V. & Wivel, H. (1998). Slag analysis as a method for the characterization and provenance of ancient iron objects, *Materials Characterization*. 40: 73-96.

[25] Kusmierek, E. & Chrzescijanska, E. (2013). Tannic acid as corrosion inhibitor for metals and alloys. *Materials and Corrosion*. 66, doi: 10.1002/maco.201307277.

[26] Barbosa, A., Jimenez, C. & Mosquera J., (2018). Detection of iron phases presents in archaeological artifacts by Raman spectroscopy, *Corrosion Science & Technology*. 17 (2): 60-67.

[27] Neff. D., Bellot-Gurlet, L., Dillmannetal, Ph., et al. (2006), Raman imaging of ancient rust scales on archaeological iron artifacts for long term atmospheric corrosion mechanisms study, *J. of Raman Spectroscopy: SI (Raman Spectroscopy in Art and Archaeology II)*. 37 (10): 1228-1237.

[28] Derrick, L., Stulik, D. & Landry, J. (1999). *Infrared spectroscopy in conservation science*, The Getty Conservation Institute, Los Angles.

[29] Abdel-Kawy, M., Ali, M. & Abdel-Maksoud, G. (2025). The effect of iron rust stains on historical papers and their removal using different cleaning methods: A review. *EJARS*. 15 (1): 1-11

[30] Senge, D. (2011). Creating a micro-climate box for metal storage, *Conserve O Gram* 4/16, National Park Service, Tucson.

[31] Mansour, M. (2018). Impact of storage conditions on biodeterioration of ancient egyptian child mummies by xerophilic fungi. EJARS 8 (2):97-107.

[32] Abu-Baker, A. & Fischer, B., (2014). Analysis and conservation of an iron dagger from tall Abu al- kharza Valley, Jordan: A case study, *MAA*. 14 (2): 365-374.

[33] Barclay, R., Dignard, C. & Selwyn, L., (2020), *Caring for metal objects*, Preventive conservation guidelines for collections online resource, Canadian conservation institute, Canada.

[34] Selwyn, L. (2004), Metals and corrosion: *A handbook for the conservation professional*, Canadian Conservation Institute, Ottawa.

[35] Rifai, M., Elshahawy, A. & Abdel Hamid, Z. (2023). Technical and conservation of a bronze mirror from Aniba, lower Nubia, *Scientific Culture*. 9 (1): 21-35.

[36] Bei, Q., Hou, B. & Zheng, M. (2013). The inhibition effect of tannic acid on mild steel corrosion in seawater wet/dry cyclic conditions, *Corrosion Science*. 72, doi: 10.1016/j.corsci.2013.01.040.